Proceedings of the 11th Brazilian Congress of Thermal Sciences and Engineering -- ENCIT 2006
Braz. Soc. of Mechanical Sciences and Engineering -- ABCM, Curitiba, Brazil,- Dec. 5-8, 2006

Paper CIT06-0270

THE USE OF THE ULTRASONIC TECHNIQUE FOR VOID FRACTION MEASUREMENTS IN AIR-WATER BUBBLY FLOWS

Áureo M. Vasconcelos
Universidade Estadual de Campinas (UNICAMP), Brazil
e-mail

Ricardo D. M. Carvalho
Universidade Federal de Itajubá (UNIFEI), Brazil
martins@unifei.edu.br

Osvaldo J. Venturini
Universidade Federal de Itajubá (UNIFEI), Brazil
osvaldo@unifei.edu.br

Fernando A. França
Universidade Estadual de Campinas (UNICAMP), Brazil
ffranca@fem.unicamp.br

Abstract. *In many industrial applications there is a need to determine the dispersed phase holdup in two-phase flows using noninvasive, fast responding techniques. Despite some limitations, ultrasonic techniques apparently can fulfill these requirements. The proposed paper describes an experimental apparatus designed specifically for the study of the ultrasonic measurement of the void fraction or gas holdup in vertical, upward air-water bubbly flows. A brief discussion of the state of the art of the ultrasonic technique as applied to the characterization of multiphase flows is also presented. Next, the two-phase flow data reduction and the ultrasonic signal processing are discussed in detail. This involves assessing the acoustic wave transit time and amplitude attenuation across the two-phase flow from the raw, digitized ultrasonic signals. Finally, the trends in the acoustic signal transit time and attenuation in the zero to 15% void fraction range are discussed. This range is typical of the bubbly flow regime, which seems to hold the greatest potential for ultrasonic measurements of the void fraction. Future research needs to improve the technique are also identified.*

Keywords*. Ultrasonic data, air-water bubbly flow, void fraction, signal attenuation, wave transit time*

1. Introduction

In many industrial applications there is a growing need for non-invasive, real-time measurement of the dispersed phase holdup in two-phase flows. Ultrasonic signals are information rich and the ultrasonic technique apparently can fulfill these requirements. The main ultrasonic parameters normally used in process monitoring, measurement, and control are the signal amplitude and the wave transit time (Bond *et al.*, 2003). In multiphase flows, as the concentration and size distribution of the dispersed media (solid particles and/or gas bubbles) change these signal properties vary due to the combined effect of acoustic attenuation and transmission phenomena.

Chang *et al*. (1982) used the ultrasonic technique for the characterization of the flow patterns of horizontal air-water two-phase flows and for the measurement of the liquid film thickness in horizontal air-mercury flows. In the former case, an emitter-receiver transducer was placed on the bottom of the flow pipe and a receiver transducer was placed on top directly across. The authors then presented and discussed the general features of the waveforms obtained from both transducers for single-phase flow of liquid and several two-phase flow patterns; they concluded that the ultrasonic technique allows for unmistakable characterization of the two-phase flow patterns. Signal processing for computation of the void fraction was not discussed.

Jones *et al*. (1986) conducted a theoretical and experimental study of the interaction of an ultrasonic wave with air-water bubbly flows. The authors claimed that a direct relationship does not exist between the ultrasonic wave attenuation and the volumetric interfacial area in a bubbly flow. Hence, if ultrasonic attenuation is to be used for the measurement of the dispersed phase holdup, some estimation of the average bubble size and shape will be necessary to permit access to the volumetric interfacial area or, likewise, the void fraction. In addition, Jones *et al*. (1986) discussed the physics involving the passage of a single bubble through the non-planar acoustic field generated by a piston-like ultrasonic source. They argued that two identical bubbles passing between the emitting and receiving transducers at different positions along the axis connecting them produce different effects. Therefore, the signals transmitted through bubbly flows are ambiguous if the bubbles are not uniformly distributed or identically distributed during the total time of measurement.

Murakawa *et al*. (2005) used two different ultrasonic transducers and statistical methods to determine the velocity distribution of bubbles in air-water bubbly flows. The investigators were then able to ascertain the effect of transducer

frequency and diameter on the accuracy of the measurement. The acoustic probe consisted of two concentric cylindrical elements with two basic frequencies, a central 8 MHz 3-mm diameter transducer jacketed by an annular 2 MHz 10-mm diameter one; the so-called Multi-Wave TDX could independently emit 2 MHz and 8 MHz ultrasonic beams. From ultrasonic pulses reflected off liquid-gas interfaces, the researchers obtained the probability density function (PDF) for all measured instantaneous velocities at each measuring position. However, the probability of bubbles crossing the ultrasonic beam becomes higher with increasing transducer diameter and, for the same flow conditions, a different profile was obtained for each transducer diameter. In this connection, Murakawa *et al*. (2005) reported an experiment in which for 3 mm to 4 mm diameter bubbles, a 2.5-mm-diameter transducer delivered data containing essentially the liquid velocity. Conversely, a 10-mm-diameter transducer provided data containing primarily the rising velocity of bubbles. Regarding single-phase flow experimentation with their own Multi-Wave TDX, the authors reported an inability to measure the liquid velocity in the near wall region due to "an overlap of the ultrasonic [beam] with the pipe wall". Supposedly, this overlap region gets wider with increasing transducer diameter. It is not clear what the authors meant by this overlap region and no further information was given.

Zheng and Zhang (2004) used the ultrasonic technique to measure the dispersed phases void fractions in three-phase and two-phase flows. Experimental results for air-oil and glass beads-oil flows indicated that gas bubbles are the dominant factor in acoustic attenuation (reduction in the response signal amplitude). However, in air-glass beads-oil three-phase flows there seems to be an interaction of the air bubbles with the glass beads so that the resulting signal attenuation is greater than the sum of the isolated effects of each one. The investigators then observed the signal attenuation to increase exponentially with increasing interfacial area of both the solid and gas phases. In addition, the air bubbles caused an increase in the acoustic wave transit time. Vatanakul *et al*. (2004) conducted an experimentation program similar to that of Zheng and Zhang (2004) using bigger glass beads. Besides confirming the observations of the latter authors, Vatanakul *et al*. (2004) also verified that the scatter in the transit time increased as the gas and solid phases holdup increased. Yet, the former had a much more pronounced and immediate effect than the latter. Regarding the signal amplitude, the scatter in the gas-liquid data rapidly increased with increasing void fraction. The opposite trend was observed for solid-liquid systems.

Despite the growing number of papers dealing with the application of the ultrasonic technique for measurements in two-phase flows, to the present authors´ knowledge a detailed discussion of the signal waveform and how it relates to the computation of the void fraction does not seem to exist. Given the complexity of the acoustic phenomena imprinted in the waveforms, the main question apparently involves which portions of the signal to consider for purposes of calculating the void fraction. The present paper addresses these issues by first describing an experimental apparatus designed specifically for the study of the ultrasonic measurement of the void fraction in vertical, upward air-water two-phase flows. Next, the two-phase flow data reduction and the ultrasonic signal processing are discussed in detail. This involves clearly identifying the acoustic phenomena imprinted in the waveforms and computing the wave attenuation and transit time across the two-phase flow from the raw, digitized ultrasonic signals. Finally, the trends in the ultrasonic parameters with increasing void fraction are compared with those reported in the literature so as to identify future research needs to improve the technique.

2. Experimental Apparatus and Procedure

2.1. Two-Phase Flow Test Rig

An experimental apparatus was designed and built specifically for the study of the ultrasonic measurement of the void fraction in vertical, upward air-water flows. Figure 1 presents a schematic view of the test rig. The air-water mixer consists of a water-filled tank where the lower end of a 54-mm inner diameter acrylic pipe is inserted. Inside this pipe there is a cylindrical porous medium through which compressed air is injected into the water flow; mixing of the air and water takes place in the annular space between the porous medium and the acrylic pipe and rapidly evolves into the bubbly flow pattern. The annular space was so designed as to guarantee a minimum liquid velocity, thus assuring an adequate and stable mixing process. Downstream of the mixer, a 3.5-m long section of the acrylic pipe assures the hydrodynamic development of the bubbly flow before it enters the void fraction measurement test section. This test section is actually a 10-cm long segment of the same 54-mm diameter acrylic pipe where the ultrasonic probes are located. In addition, a variable reluctance pressure transducer tapped just downstream of the ultrasonic probes measures the flow pressure; this reading is necessary for the calculation of the air flow rate under actual test conditions. The acrylic piping just bellow the test section is surrounded by a water-filled transparent square box, making it possible visual observations and fast moving filming of the bubbly flow. Following the test section a 1.6-m long portion of the acrylic pipe discharges the air-water two-phase flow in a phase separator. A quick valve device installed in this part of the flow loop allows for measurements of the volumetric void fraction, which can be used to corroborate the results from the ultrasonic probes.

In the separator the air is vented into the atmosphere while the gravity driven water flow returns to the liquid reservoir. A centrifugal pump then forces the water back to the air-water mixer, thus closing the flow loop. A variable speed driver allows for a zero to 5,000 kg/hr water flow rate variation. The water flow rate is measured by model Rheonik RHM12 Coriolis-type flow meter, which includes an RTD for temperature measurements. The air flow rate is

measured by models 50MJ10-9 and 50MJ10-12 Meriam Instruments laminar flow elements. Model PX 750 Omega pressure transducers, ranging from 0 to 700 mmH_2O, are used to measure the pressure difference across the laminar flow elements. An identical pressure transducer, tapped just downstream the laminar flow elements, reads the gage air flow pressure. Atmospheric pressure measurements come from the University weather station, reported continuously through Internet. A type J thermocouple measures the flowing air temperature. Bourdon type manometers and thermocouples permit double checks on these automatic digital measurements as well as direct visual monitoring of the flow loop proper operation. Values of the flow loop operating parameters are then entered into a Microsoft Excel spreadsheet that calculates the actual air flow rate at the test section and the air and water superficial velocities. The void fraction results for the same operating conditions, as reported by Dias *et al* (2000), are then entered into the spreadsheet, as well as the ultrasonic wave amplitude attenuation and transit time, provided by the signal-processing algorithm.

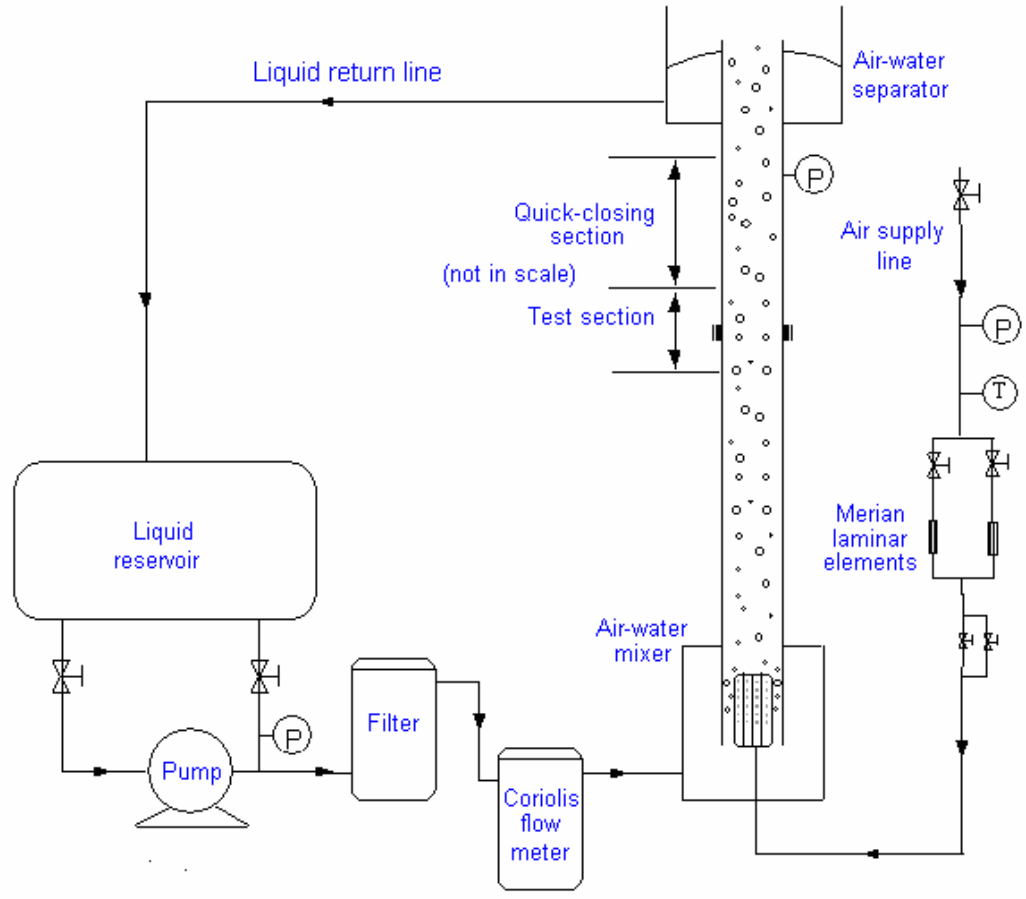

Figure 1. Schematic view of the air-water bubbly flow test rig.

2.2. Ultrasound Instrumentation

Figure 2 shows a schematic view of the test section instrumentation. Two plexiglass adapters were curve machined on one side so as to be snugly fitted to the outer surface of the plexiglass pipe. The emitter and receiver ultrasonic transducers were then fixed to the opposite surfaces of these plexiglass blocks; a thin gel layer was applied to the transducers front surface before mounting to enhance mechanical contact. The emitter-receiver ultrasonic path is then made of a 10-mm long distance across each acrylic block, a 3-mm long acrylic pipe wall crossing on each side, and the 54-mm pipe inner diameter. In other words, the ultrasonic total path length consists of a 13-mm segment across the acrylic on the emitter side, a 54-mm crossing of the two-phase flow, and a 13-mm segment across the acrylic on the receiver side. In checking the ultrasonic wave transit time, to be discussed later, the gel layer thickness was neglected.

The emitter and receiver transducers generated 2.5 MHz ultrasonic pulses, within the range of water-transmitted signals. The transducers were driven by a Panametrics 5072 Pulser-Receiver, which in turn was connected to a National Instruments PXI data acquisition system. The PXI is a Windows based industrial PC with chassis slots for board insertion. The PXI system was used for data acquisition, storage, and transfer and for process monitoring through a virtual oscilloscope. A supervisory system based on the LabView software was used to perform these tasks. To acquire the data, a 100 MHz maximum capability sampling board was used.

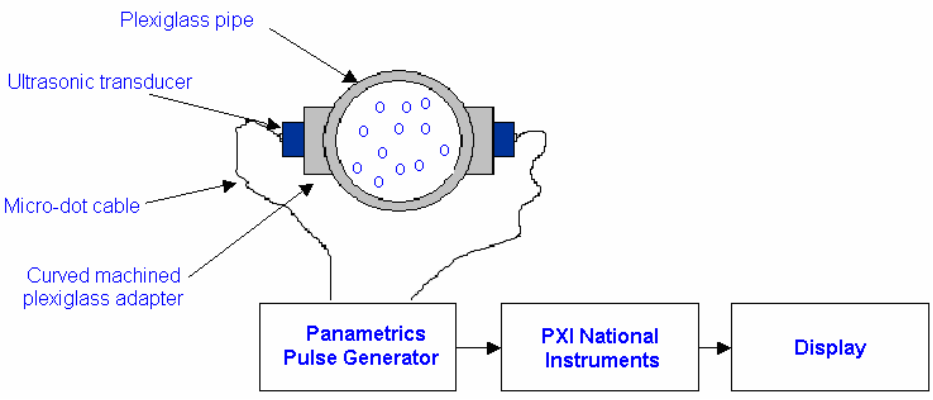

Figure 2. Schematic view of ultrasonic instrumentation assembly.

2.3. Experimental Procedure

In selecting air and water flow rates to be tested, the sampling frequencies, and the 5072 PR pulsing frequency, the following criteria were adopted:

1. Void fraction values should span the zero to 15% range, characteristic of the bubbly flow regime, and specific values should be as close as possible to those tested by Dias *et al* (2000) using the same test rig. Hence, independent measurements of the mean void fraction, mean bubble diameter, interfacial area density and void fraction distribution would be available for reference.
2. Sampling frequencies of the ultrasonic signals should be high enough to avoid alias and to allow for accurate determination of the ultrasonic wave transit time. Additionally, the samples should contain enough information for an analysis of the signal frequency spectrum; this study is intended to investigate possible modifications to the transmitted pulse frequency composition by the two-phase flow.
3. The pulsing frequency should be such that a statistically significant number of pulses is contained in each sample.

According to these criteria the sampling frequencies selected were 20 and 100 MHz, far greater than the ultrasonic transducers intrinsic frequency and the two-phase flow stochastic fluctuations. Given the PXI system 600,000 data points maximum storage capacity, the sampling periods corresponding to the 20 and 100 MHz frequencies were 0.030 and 0.006 seconds, respectively. The 5072 PR pulsing frequency was set at 2.5 kHz so that each 20 MHz and 100 MHz sample contained 75 and 15 pulses, respectively. For each void fraction value, the acoustic signal was sampled at least twice. Even though the number of pulses in the 100 MHz samples is rather low, these are intended mainly for a study of the signal spectral makeup and an assessment of the error in the acoustic wave transit time.

Finally, in order to use the ultrasonic technique for void fraction measurements a reference is needed with which to compare the response signal attenuation across the two-phase flow. One possible reference would be the emitter signal itself; however, this approach would make signal processing cumbersome and dependent on specific settings of the 5072 PR. A more practical approach reported in the literature (Vatanakul *et al*., 2004; Zheng and Zhang, 2004) is to use as reference the response signal for the single-phase flow of the continuous phase. In the present case, preliminary tests showed that the water superficial velocity and temperature have no significant effect on the acoustic signal attenuation. Therefore, it was decided that reference signals would be obtained for single-phase still water ($j_{air} = j_{water} = 0$) in the test rig immediately before any run of tests. One can thus be sure that secondary variables such as minor adjustments in the transducers position are always taken into account.

3. The Acoustic Wave Equation and Basic Acoustic Parameters

Before proceeding to discuss the ultrasonic signals obtained in the current investigation, a brief review of acoustics theory is in order. The motion associated with the vibration of simple mechanical systems or with the propagation of simple sound waves in a fluid medium is often oscillatory in nature. This simple harmonic motion is described mathematically by a sine and/or cosine function as depicted in Figure 3. The wavelength λ and period T are related by,

$$\lambda = c\,T \tag{1}$$

where *c* is the wave phase speed. Another important parameter is the wave number *k*, which represents the number of wave crests per unit distance in the direction of propagation. Mathematically, it given by the ratio between the wave angular frequency, ω, and the wave speed, c,

$$k = \frac{\omega}{c} \tag{2}$$

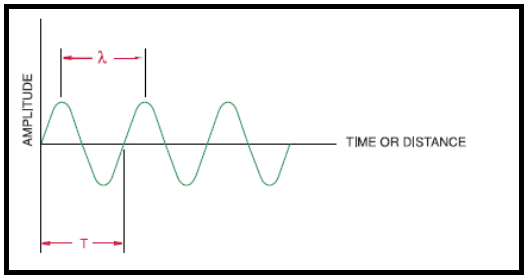

Figure 3. Simple harmonic motion.

The simplest case of acoustic analysis is that involving plane waves, that is, waves for which each acoustic variable (particle displacement, density, pressure, etc.) has constant amplitude on any given plane perpendicular to the direction of wave propagation. The analysis that follows is based mostly on Kinsler *et al*. (2000). If the plane wave propagates along the *x* axis, the linearized, lossless wave equation for the propagation of sound in fluids reduces to,

$$\frac{\partial^2 p}{\partial x^2} = \frac{1}{c^2}\frac{\partial^2 p}{\partial t^2} \tag{3}$$

where $p = f(x, t)$ is the excess pressure or *acoustic pressure* and c is the wave phase speed. The acoustic pressure is the difference between the instantaneous pressure at any point and the constant equilibrium pressure in the fluid. In this equation the effects of gravitational forces were neglected so that equilibrium values of fluid density and pressure can be assumed uniform throughout the fluid; in addition, the wave is supposed to be of relatively small amplitude so that changes in density will be small compared to the equilibrium value. Finally, dissipative effects such as those arising from viscosity or heat conduction are also neglected.

The complex form of the harmonic solution for the acoustic pressure of a plane wave is,

$$\tilde{p} = \tilde{C}_1 \exp[j(\omega t - kx)] + \tilde{C}_2 \exp[j(\omega t + kx)] \tag{4}$$

where the symbol ~ denotes a complex quantity. The associated velocity particle velocity is entirely in the direction of propagation and is given by,

$$\tilde{u} = \frac{\tilde{C}_1}{\rho_o c}\exp[j(\omega t - kx)] + \frac{\tilde{C}_2}{\rho_o c}\exp[j(\omega t + kx)] \tag{5}$$

The energy transported by acoustic waves through a fluid medium is of two forms; the kinetic energy of the moving particles and the potential energy of the compressed fluid. The total acoustic energy of a fluid element of undisturbed volume V_0 is then given by,

$$E = E_k + E_p = \frac{1}{2}\rho_o\left(u^2 + \frac{p^2}{\rho_o^2 c^2}\right) \tag{6}$$

The acoustic intensity *I* of a sound wave is defined as the average flow rate of energy through a unit area normal to the direction of propagation. The instantaneous rate at which work is done per unit area by one element of fluid on an adjacent element is *pu*. The intensity is the time average of this rate,

$$I = < p\,u >_t = \frac{1}{t}\int_0^t p\,u\,dt \tag{7}$$

where the integration is taken over a time corresponding to the period of one complete cycle. To evaluate this integral for any particular wave, it is necessary to know the relationship between *p* and *u*. For plane harmonic waves, one gets,

$$I_{\pm} = \pm \frac{P_e^2}{\rho_o c} \tag{8}$$

for a plane wave traveling in either the $+x$ or $-x$ direction. The quantity P_e is the *effective amplitude of acoustic pressure* given by,

$$P_e = \frac{P}{\sqrt{2}} \tag{9}$$

The *specific acoustic impedance* is defined as,

$$\tilde{z} = \frac{\tilde{p}}{\tilde{u}} \tag{10}$$

For plane waves this ratio becomes,

$$\tilde{z} = \pm \rho_o c \tag{11}$$

The plus or minus sign depends on whether propagation is in the plus or minus direction. The product $r = \rho_o c$ is a characteristic property of the medium referred to as the *characteristic impedance (resistance)* of the medium. Although the specific acoustic impedance of the medium was found to be a real quantity for progressive plane waves, in the general case it is a complex quantity.

When an acoustic wave propagating in one medium hits the boundary of a second medium, reflected and transmitted waves are generated. The ratios of the pressure amplitudes and intensities of the reflected and transmitted waves to those of the incident wave depend on both the characteristic acoustic impedances and speeds of sound in the two media and on the angle the incident wave makes with the normal to the interface. For plane waves transmitted from one fluid to another at normal incidence, the *pressure transmission and reflection coefficients* can be shown to be,

$$\tilde{R} = \frac{1 - \frac{r_1}{r_2}}{1 + \frac{r_1}{r_2}} \tag{12}$$

$$\tilde{T} = \frac{2}{1 + \frac{r_1}{r_2}} \tag{13}$$

The *intensity reflection and intensity transmission coefficients* of plane waves are then given by,

$$R_I = \left(\frac{1 - \frac{r_1}{r_2}}{1 + \frac{r_1}{r_2}} \right)^2 \tag{14}$$

$$T_I = 4 \frac{\frac{r_1}{r_2}}{\left(1 + \frac{r_1}{r_2} \right)^2} \tag{15}$$

Since for normal incidence the cross-sectional areas of all acoustic beams are equal, the *power coefficients* are equal to the intensity coefficients.

Interface transmission and reflection phenomena are complicated when one of the media is a solid; however, for normal incidence a large class of solids obeys the same equations developed for fluids. The only modification needed is that the speed of sound in the solid must be based on the bulk modulus. Furthermore, for relatively rigid nonporous solids such as steel, glass, and so forth with transverse dimensions much larger than the wavelength of the impinging acoustic wave, two types of elastic waves may be propagated, plane longitudinal and plane shear waves. For oblique incidence, the incident wave may be refracted into longitudinal bulk waves traveling in one direction and transverse shear waves traveling at a lower speed in a different direction.

Table 1 shows numerical values for the basic acoustic parameters for the present test rig. Table 2 presents values for the transit time along the ultrasonic path discussed in Sec. 2.2 (*Ultrasound Instrumentation*); calculations were made considering only single-phase flow of water.

Table 1. Numerical values for the acoustic parameters in the present test rig.

Material or Interface	**Longitudinal Velocity [m/s]**	**Shear Velocity [m/s]**	**Characteristic Impedance [kg/m^{2}s x 10^6]**	$\tilde{R}$	$\tilde{T}$	R_I	T_I
Acrylic Resin	2,730	1,430	3.22	-	-	-	-
Water at 20°C	1,480	-	1.48	-	-	-	-
Acrylic / Water	-	-	-	- 0.37	0.63	0.14	0.86
Water / Acrylic	-	-	-	0.37	1.37	0.14	0.86

Table 2. Ultrasonic waves transit time in the test rig.

Wave	**Transit Time [μsec]**			
	First Adapter/Tube Wall	Water	Second Adapter/Tube Wall	Total
Longitudinal	4.8	36.5	4.8	46.0
Transverse	-	-	9.1	9.1

4. Signal Analysis

Figure 4 shows a typical trace signal of the ultrasound emitter-receiver assembly as the bubbly air-water flow goes through the ultrasonic field. The signal amplitude in the y-axis is related to the ultrasonic field intensity at the receiver position; its absolute value, however, is affected by the amplification of the instrumentation electronics. The “bang”, which corresponds to a pulse of the Panametrics 5072 Pulse-Receiver, can be unmistakably identified as an outstanding isolated peak. Although its time of occurrence is correctly detected by the particular setting of the ultrasound instrumentation, its amplitude in Figure 4 does not correspond to the intensity of the actual pulse generated by the pulse-receiver; the isolated peak can be more appropriately interpreted as an electronic noise surge at the moment the actual pulse is generate. Next, a sequence of peaks and valleys is the receiver response to the ultrasonic pulse attenuated by and transmitted through the air-water bubbly mixture and plexiglass elements. Finally, there seems to be a small-scale version of these same peaks and valleys hitting the receiver some time after the first sequence. For computer calculations purposes, the moment the ultrasonic wave hits the receiver transducer was taken as when the voltage signal starts decreasing monotonically beyond an appropriate threshold value selected to distinguish it from the base noise. This corresponds to the beginning of the first incoming pulse. The time interval between the bang and the signal arrival at the receiver transducer is the ultrasonic wave transit time and can be easily calculated by counting the number of data points between them.

Although the calculation of the wave transit time was fairly straightforward, the characterization of the received signal amplitude was not so obvious. In this regard, it was experimentally observed that the first valley in the first incoming pulse was much more sensitive to void fraction variations than the first peak in the same sequence (Figure 5). As to the second sequence of peaks and valleys, it exists only for the single-phase flow of water and very low void fraction bubbly flows (Figure 6 and Figure 7). Collected data showed it hits the receiver transducer approximately 8.7 μsec after the first sequence, which agrees very closely with the 9.1 μsec shear wave transit time in the second adapter / tube wall assembly (Table 2). It was, therefore, disregarded as a measure of the dispersed phase holdup. The amplitude of the received signal was then somewhat arbitrarily taken as that of the first valley immediately following the signal arrival; mathematically it is identified as an inflection point.

In an attempt to gain a deeper understanding of the ultrasonic signals obtained, the likelihood of the entire first sequence of peaks and valleys to be related to the void fraction was also checked. It can be observed in Figure 5 that the time for the signal response to die out does not seem to depend on the void fraction (2.4 μsec for $\alpha = 0\%$; 2.7 μsec for $\alpha = 2.9\%$, 2.4 μsec for $\alpha = 6.1\%$; and 2.2 μsec for $\alpha = 10.9\%$). As will be seen later, this behavior is in agreement with the

fact that the variation in the transit time with void fraction was very small (Figure 8). On the other hand, the amplitude of the peaks and valleys changes considerably with void fraction, which means that the energy contained in the signals also changes. Hence, in spite of amplification by the electronics, the energy contained in the whole sequence of peaks and valleys should be linked to the energy transported by the acoustic wave, Eq. (6), and, thus, reflect the interaction between the wave and the bubbly mixture. The following equation was used to obtain the energy in the received signal as it appears in the data samples,

$$E = \int |A|^2 \, dt \tag{16}$$

In the computer routine, this equation was replaced with a summation of the squared amplitude through the duration of the digitized signal.

The signal processing thus yields three acoustic parameters that can tentatively be correlated with the void fraction, namely, the wave transit time, the received signal amplitude and energy, as defined above. A computer algorithm was then written using MATLAB software to recognize the emitter pulse based on an appropriate voltage level threshold and to calculate the wave transit time, the receiver response amplitude and energy. All the results for the signal amplitude and energy were normalized using the corresponding results for single-phase still water as reference (Sec. 2.3, *Experimental Procedure*). In addition, as each sample contains several pulses, basic statistics associated with the acoustics parameters are also calculated. In this regard, in Figure 6 and in Figure 7 the response signals to 75 pulses were overlaid so that the signal consistency could be assessed. As can be seen, all trace signals are alike, which testifies to the reliability of the instrumentation used.

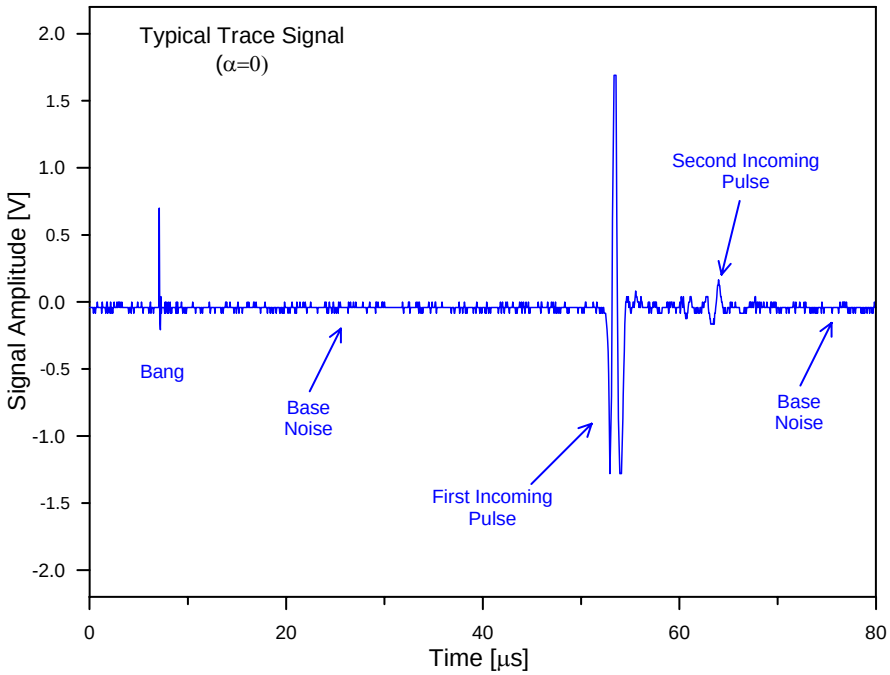

Figure 4. Trace signal of the ultrasonic emitter-receiver assembly for α = 0%.

5. Experimental Results

Ultrasonic data were collected for void fractions in the zero to 15% range, characteristic of the bubbly flow regime in the air-water vertical flow rig. In order to digitize the ultrasonic signals 20 and 100 MHz sampling frequencies were used. Figure 8 presents the transit time variation as a function of the void fraction for all data samples. Once again, the experimental results for single-phase water (around 44.9 μsec) are in close agreement with the 46.0 μsec calculated value in Table 2. The overall variation in the transit time throughout the zero to 12% void fraction range stayed within 0.5 μsec, and the correlation coefficient was 0.81 for both the 20 MHz and the 100 MHz series. This indicates a fairly strong correlation between the transit time and the void fraction. The standard deviations were very small for all samples, representing only 0.3% or less of the mean value; however, even these small standard deviations represented a significant fraction of the 0.5 μsec overall variation. Therefore, the increase in the transit time due to dispersive wave propagation does not seem to provide sufficiently reliable measurements of the void fraction in industrial applications.

Figure 9 shows the signal amplitude ratio as a function of the void fraction. As expected, the amplitude ratio decreases with increasing void fraction; however, the 100 MHz sampling frequency series exhibits a greater scatter than the 20 MHz one. In this connection, at 100 MHz sampling frequency only one-fifth of the acoustic pulses can be

acquired compared to the 20 MHz samples. Hence, the two-phase flow stochastic fluctuations are not well represented (and smoothed out) in the 100 MHz samples and the resulting mean values are less significant. The values of the correlation coefficients were 0.91 and 0.84 for the 20 MHz and 100 MHz series, respectively. Even if the acoustic attenuation phenomena are not completely represented in the first response signal valley, these values for the correlation coefficient still indicate a strong correlation between the amplitude ratio so defined and the void fraction.

Figure 10 shows the amplitude ratio standard deviation as a function of the void fraction. In general, there is a decrease in the standard deviation as the void fraction increases, which could be explained by a great sensitiveness of the acoustic attenuation phenomena to instantaneous variations in the number of bubbles per unit volume and, consequently, the bubbles interfacial area density. In some cases, the standard deviation attained as much as 40% of the mean value. One should bear in mind, though, that Vatanakul *et al.* (2004) reported a five-fold in the amplitude ratio standard deviation as the void fraction increased from zero to approximately 7% for gas-liquid data. A physical explanation for this behavior was not put forth by the authors.

Figure 11 displays the mean energy in the response signal samples as a function of the void fraction. As was the case with the amplitude ratio, the signal energy decreases rapidly as the void fraction increases. The values of the correlation coefficients were 0.90 and 0.83 for the 20 MHz and 100 MHz series, respectively, essentially the same as those found for the signal amplitude ratio. Therefore, further study is necessary before a decision can be made regarding which acoustic parameter, the energy or the amplitude, is more representative of the interaction of the ultrasonic wave and the two-phase flow for purposes of measuring the void fraction.

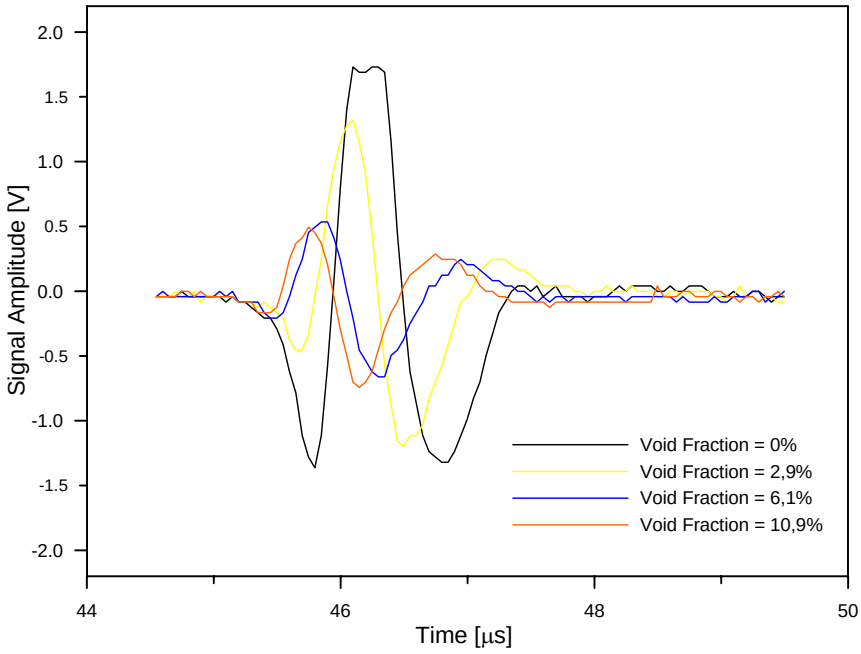

Figure 5. Response signal duration for increasing void fraction values.

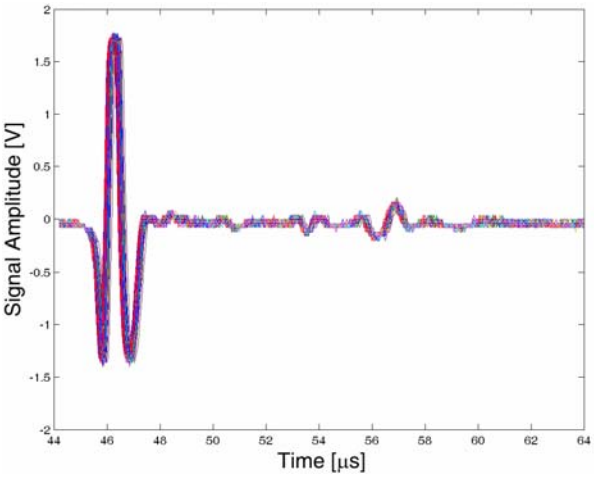

Figure 6. Response signals (20 MHz, j_{water} = 0, and α=0%).

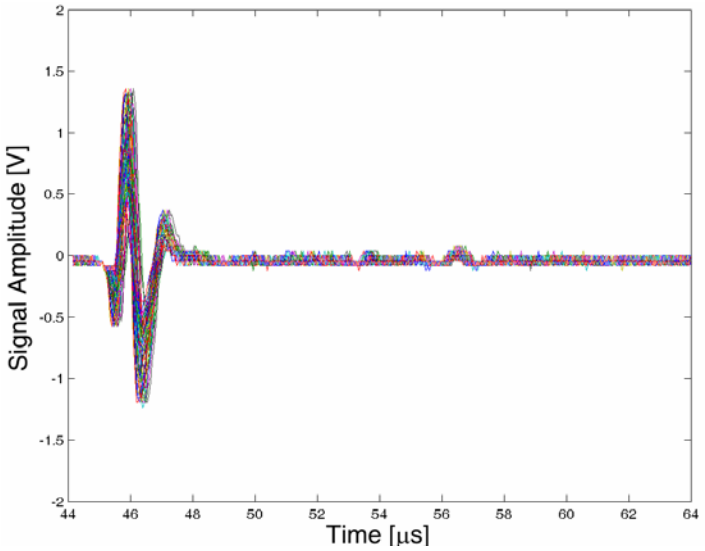

Figure 7. Response signals (20 MHz, j_{water} = 0, and α=2.9%).

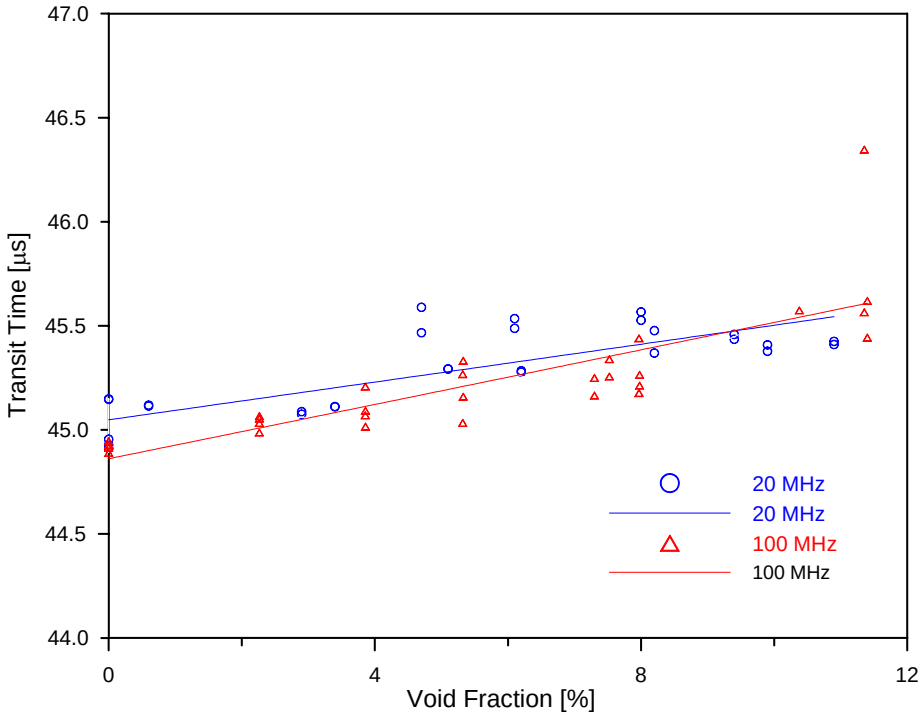

Figure 8. Transit time as a function of void fraction.

6. Conclusions

A two-phase flow test rig was built and instrumented with ultrasonic transducers. Ultrasonic data were then collected for the zero to 15% range, characteristic of bubbly flow pattern in this experimental set-up. The basic features of the trace signals were clearly identified, namely, the pulse generated at the emitter transducer ("bang") and the longitudinal wave and shear wave response signals at the receiver transducer.

The ultrasonic parameters calculated for the longitudinal wave response signal were the transit time, amplitude, and energy. Reduced data exhibited the expected behavior; as the void fraction increased the transit time increased while the amplitude and energy decreased. Whereas the transit time variation seems too small to be reliably used as a measure of the void fraction, the amplitude and energy attenuation apparently are suitable for this purpose. However, further work is necessary in order to better understand the interaction of ultrasonic waves with two-phase flows.

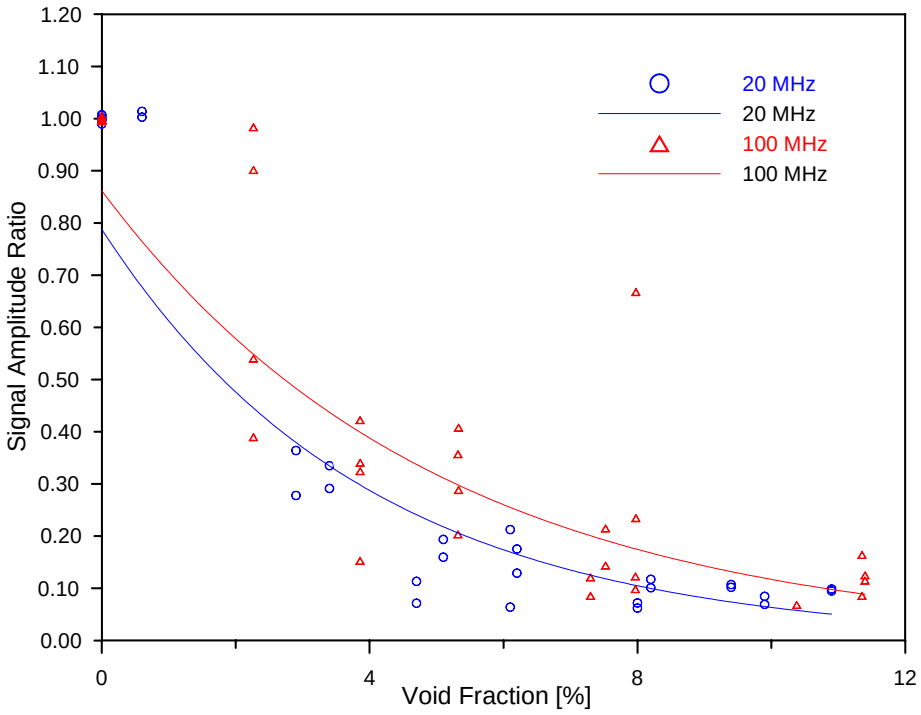

Figure 9. Response signal amplitude ratio as a function of void fraction.

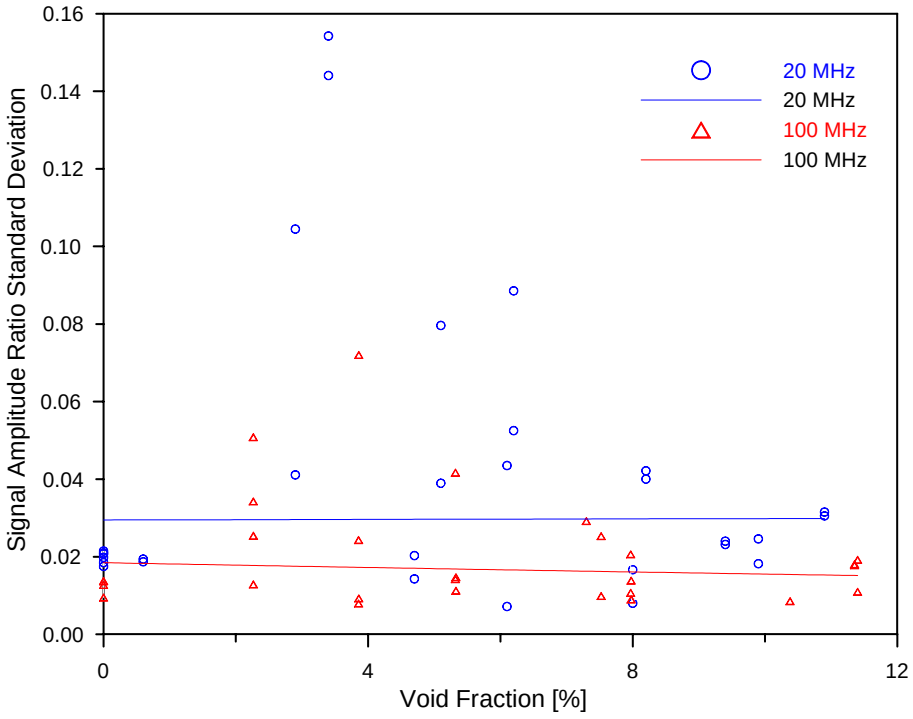

Figure 10. Response signal amplitude ratio standard deviation as a function of void fraction.

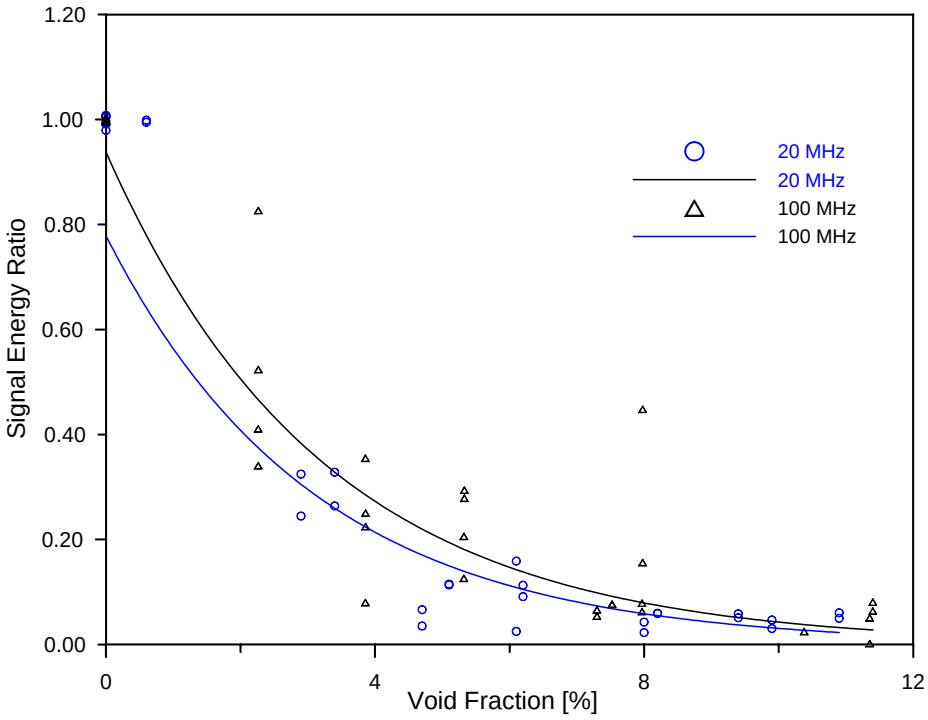

Figure 11. Response signal mean energy as a function of void fraction.

7. Acknowledgements

The authors wish to acknowledge the financial support received from PETROBRÁS, the Brazilian National Petroleum Company, which made possible this study.

8. References

Bond, L. J., Morra, M., Greenwood, M. S., Bamberger, J. A., and Pappas, R. A., 2003, *Ultrasonic Technologies for Advanced Process Monitoring, Measurement, and Control* Proceedings 20th IEEE Instrumentation and Measurement Technology Conference, Vail, CO, USA.

Chang, J. S., Ichikawa, Y., and Irons, G. A., 1982, *Flow Regime Characterization and Liquid Film Thickness Measurment in Horizontal Gas-Liquid Two-Phase Flow by an Ultrasoinc Method*, AIAA/ASME Joint Plasma Thermophysics HTC.

Dias, S, França, F. A., and Rosa, E. S., 2000, *Statistical Method to Calculate Local Interfacial Variables in Two-Phase Bubbly Flows Using Intrusive Crossing Probes*, International Journal of Multiphase Flow, Vol. 26 (11), pp. 1797-1830.

Jones, S. W., Amblard, A., and Favreau, C., 1986, *Interaction of an Ultrasonic Wave with a Bubbly Mixture, Experiments in Fluids*, Vol. 4, pp. 341-349..

Kinsler, L. E., Frey, A. R., Coppens, A. B., Sanders, J. V., 2000, Fundamentals of Acoustics, John Wiley & Sons, Inc., Fourth Edition.

Kumar, M., and Horne, R. N., 2003, *Ultrasonic Rate Measurements in Two-Phase Bubble Flow*, SPE Annual Technical Conference and Exhibition, Dallas, USA.

Murakawa, H., Kikura, H., and Aritomi, A., 2005, Application of Ultrasonic Doppler Method for Bubbly Flow Measurement Using Two Ultrasonic Frequencies, Experimental Thermal an Fluid Science, Vol. 29, pp. 843-850.

Vatanakul, M., Zheng, Y., and Couturier, M., 2004, *Application of Ultrasonic Technique in Multiphase Flow*, Industrial and Engineering Chemistry Research., Vol. 43, pp. 5681-5691.

Zheng, Y., and Zhang, Q., 2004, *Simultaneous Measurement of Gas and Solid Holdups in Multiphase Systems Using Ultrasonic Technique*, Chemical Engineering Science, Vol. 59, pp. 3505-3514.

9. Copyright Notice